

HLRZ 95-73  
WUB 95-44

# First Lattice Study of Ghost Propagators in SU(2) and SU(3) Gauge Theories<sup>†</sup>

H. Suman<sup>‡</sup>

*Fachbereich Physik, University of Wuppertal,  
Gaußstr. 20, 42097 Wuppertal, Germany*

K. Schilling

*HLRZ c/o KFA Jülich, 52425 Jülich, Germany  
and DESY, Hamburg, Germany*

## Abstract

We present a numerical study of the ghost propagators in Landau gauge for SU(2) and SU(3) gauge theories at  $\beta=2.7$  and  $\beta=6.0$ , respectively. Analyzing different lattice sizes up to  $32^4$ , we find small finite size effects. Down to the smallest available momenta, we observe no evidence for dipole behaviour of the ghost propagators.

## 1 Introduction

The gluon propagator,  $P$ , albeit a non-gauge-invariant quantity, is considered of prime interest in the quest to gain intuitive insight into the physics of confinement in non-Abelian gauge theories. From a linearly rising potential, one would argue that  $P$  is dominated by a  $1/p^4$  singularity[1]. This infrared behaviour can be drastically altered, however, in a scenario of dynamical gluon mass generation as pointed out in Ref.[2].

The issue is closely related to the singularity structure of the Green function of the Faddeev-Popov ghost. In his seminal paper on gauge fixing ambiguities GRIBOV [3] has dealt with the implications of the proper choice of integration range (in the functional gauge field integrals) onto the singularity structure of the ghost propagator. This is elaborated in detail in a recent comprehensive

---

<sup>†</sup>We acknowledge A. Hulsebos who contributed substantially during the early stages of this work.

<sup>‡</sup>On leave from the Energy Research Group, University of Damascus, Syria.

paper by ZWANZIGER [4] where the theoretical arguments are presented in quite some detail that lead up to the prediction of a dipole-type infrared singularity in the Faddeev-Popov propagator.

It is well accepted by now that the lattice laboratory provides a valuable tool to the heuristic study of this highly intricate non-perturbative scenario. Indeed, lattice investigations of the gluon propagator in Landau gauge did reveal a momentum dependent effective mass for the gluon[5, 6]. It should be remembered, though, that – in view of the very Gribov ambiguities – such lattice results rely deeply on the quality and efficiency of gauge fixing procedures on the lattice [6, 7].

In this letter, we wish to complement the previous gluon propagator investigations by presenting a first numerical study of the ghost propagator via direct lattice simulation.

## 2 Faddeev-Popov Operator

The ghost fields can be defined on the lattice\* in a similar manner as in the continuum. The ghost propagator  $G$  is given in terms of the inverse of the Faddeev-Popov operator  $M$ :

$$M = -\nabla D(U), \quad (1)$$

where  $D(U)$  stands for the covariant derivative on the lattice. It has a diagonal form in the algebra space, being an average over field configurations:

$$G(x - y)\delta^{ab} \equiv \langle M^{-1}{}^{ab}(x, y) \rangle. \quad (2)$$

In a Landau gauge fixed configuration the action of the operator  $M$  on an arbitrary element  $w$  in the algebra space  $\mathcal{A}$  of the gauge group  $SU(N)$  is given by

$$\begin{aligned} (M\omega)^a(x) = & \sum_{\mu} \left\{ S_{\mu}^{ab}(x) [\omega^b(x) - \omega^b(x + \hat{\mu})] - (x \leftrightarrow x - \hat{\mu}) \right. \\ & \left. - \frac{1}{2} f^{abc} [A_{\mu}^b(x)\omega^c(x + \hat{\mu}) - A_{\mu}^b(x - \hat{\mu})\omega^c(x - \hat{\mu})] \right\}. \end{aligned} \quad (3)$$

Here  $S$  is a linear functional

$$S_{\mu}^{ab}(x) = -\frac{1}{2} \text{Tr} \left[ (\tau^a \tau^b + \tau^b \tau^a) (U_{\mu}(x) + U_{\mu}^*(x)) \right]. \quad (4)$$

$A_{\mu}^a$  is the gluon field and the Pauli matrices  $\tau$  are used to span an antihermitian basis of the linear space  $\mathcal{A}$ .

---

\*A very useful collection of the relevant lattice formula related to the ghost fields can be found in Ref. [4].

### 3 The Simulation

**Run Parameters.** We ran simulations on a series of lattices, whose parameters are summarized in Table 1.

	size	$\beta$	# Configurations
SU(2)	$16^4$	2.7	50
	$32^4$	2.7	15
SU(3)	$8^4$	6.0	64
	$16^3 \times 32$	6.0	30
	$24^4$	6.0	10

Table 1: *Lattices used in this simulation.*

The SU(2) gauge configurations were generated using the Kennedy-Pendleton heatbath algorithm. 2000 updates were discarded for thermalization, while gauge fixing and ghost propagator calculations took place every 100 updates. For SU(3), we applied a hybrid algorithm of Cabibbo-Marinari heatbath and Creutz overrelaxation steps with mixing probability 1:5. The configurations have been analyzed every 250 sweeps after 2000 thermalization steps.

**Gauge fixing.** Gauge fixing was done by minimizing the functional

$$F_U[g] = \sum_x \sum_\mu \left( 1 - \frac{1}{N} U_\mu^g(x) \right); \quad U_\mu^g(x) = g(x) U_\mu(x) g^\dagger(x + \hat{\mu}). \quad (5)$$

This lattice condition is slightly stronger than the conventional Landau condition in continuum theory:

$$\partial_\mu A^\mu = 0. \quad (6)$$

The minimization procedure may be carried out by use of one of the standard relaxation algorithms which will drive the system to one of its local minima of  $F_U[g]$ , thus delivering one of the possible Gribov copies.

We aim to achieve configurations lying in the fundamental modular region  $\Lambda$ , which is given by the set of absolute minima of  $F_U[g]$  on all gauge orbits. The way to do that is to modify the gauging algorithm and to mobilize the system such as to allow – in a gentle manner – for escape from the attraction of its current closest minimum. To that end we applied two approaches: (a) the simulated annealing (SA) for SU(2) and (b) the stochastic overrelaxation (SOR) algorithms for SU(3):

(a) The idea of the annealing algorithm is most easily exposed in the language of spin models: Minimizing  $F_U[g]$  may be viewed as retrieving the ground state of a spin system, with action being given by

$$S_U(g) = -\beta_s F_U[g]. \quad (7)$$

In this picture, the ground state may be reached by performing Monte Carlo sweeps on the ‘spin’ degrees of freedom  $g$ .

Let us give our prescripton of the annealing algorithm in detail: (1) start at a spin model coupling  $\beta_s = 0.20$ , and perform 10 Creutz or Kennedy-Pendleton heatbath updates on the spin model, at given  $\beta_s$ ; (2) increase  $\beta_s$  in steps of  $\Delta\beta_s = 0.20$  and keep updating until  $\beta_s = 25.0$  is reached; (3) at this point turn to ordinary relaxation.

This gauging procedure was found to be very efficient on both  $16^4$  and  $32^4$  lattices.

(b) In the stochastic overrelaxation, a “wrong” gauge transformation is applied once in a while, i.e. with probability  $w$ , during the iteration process. If  $w$  is sufficiently high, the system may be driven away from a local minimum. We applied this method in conjunction with the Los Alamos algorithm [8] after mapping the lattice onto a checker board basis. We have set the probability  $w=0.7$ . Our criterion for achieving the Landau condition was

$$|\partial_\mu A^\mu|^2 < 10^{-6}. \quad (8)$$

On our largest SU(3) lattice,  $24^4$ , about 1200-1400 iterations were needed.

**Inversion of  $M$ .** In Landau gauge,  $M = -\nabla D = -D\nabla$  is a singular matrix. It annihilates all zero modes on the left and on the right hand sides. Therefore, in order to compute its inverse, we have to separate the zero modes and perform the inversion on its regular part only.  $M$  is a real symmetric matrix acting on the algebra space  $\mathcal{A}$  of the gauge group, which may be decomposed into two subspaces:

$$\mathcal{A} = \mathcal{A}_0 \oplus \mathcal{A}_1 \quad (9)$$

such that

$$M \mathcal{A}_0 = 0 \quad \text{and} \quad M \mathcal{A}_1 \neq 0 \quad (= 0 \text{ only for the null vector}). \quad (10)$$

We start with the simple observation that the vector  $Mv$  lies in  $\mathcal{A}_1$  for arbitrary  $v$  and compute  $G$  by solving the linear equation

$$M M v = M s, \quad (11)$$

using the conjugate gradient (CG) and minimal residuum (MR) as standard iterative algorithms. Both methods start off from some initial guess vector  $v_0$  and achieve an improved approximation to the solution by adding a vector  $dv_i$  to the current value  $v_i$  at each iteration step:  $v_i \rightarrow v_{i+1} = v_i + dv_i$ . Since Eq. 11 ensures that both the starting vector and the source belong to  $\mathcal{A}_1$ ,  $v_i$  and  $dv_i$  will lie also in  $\mathcal{A}_1$ . The iteration will therefore converge to the unique solution within  $\mathcal{A}_1$ .

The solution we obtain in this manner coincides with the ghost propagator restricted to the subspace  $\mathcal{A}_1$  orthogonal to the zero modes. Hence, we can study its behaviour in momentum space, down to (and including) the smallest non vanishing momentum,  $p_{min} = 2\pi/L$ .

## 4 Results

We calculate the ghost propagators on local sources at  $x_0 = (\frac{L}{2}, \frac{L}{2}, \frac{L}{2}, 0)$  and choose the arbitrary normalization  $G(x_0)=1$  on the lattices quoted in Table 1. Then we perform the Fourier transforms, for different values of lattice momenta:

$$G(p) = \sum_x G(x) e^{-ip_\mu(x_\mu - x_\mu^0)}, \quad p_\mu = \frac{2\pi}{L} k_\mu, \quad k_\mu = 0, \dots, L-1. \quad (12)$$

In the practical implementation, we keep two components at  $k_\mu = 0$ , and vary the remaining two components, covering their entire available kinematical range.

Figure 1 shows the resulting propagators  $G(p)$  in the case of SU(3), for the lattices  $8^4$ ,  $16^4$ ,  $16^3 \times 32$ , and  $32^4$ . The abscissa is given in terms of the appropriate lattice momentum  $q$

$$q(p) = 2 \sqrt{\sum_\mu \sin^2\left(\frac{p_\mu}{2}\right)}. \quad (13)$$

Some observations can be made from the ghost propagators in momentum space:

1. On a given lattice the fluctuations of the data points appear to be small. In the presence of Gribov copies, however, one would expect to encounter large fluctuations due to gauge dependence. We therefore conclude that we should not worry about Gribov copies.
2. On the different lattices all data points above  $p_{min} = 2\pi/L$  collapse nicely to a universal curve. Notice in particular the near-coincidence of the two points at  $p=2\pi/16$  which are measured in the short and long direction of the  $16^3 \times 32$  lattice.

Looking at the smallest lattice  $8^4$ , we find the data point  $G(p=2\pi/8)$  to lie above the corresponding point from the  $24^4$  lattice by several standard deviations. This tells us that finite size effects shift  $G$  upwards rather than downwards.

3. Down to the smallest momentum on the  $24^4$  lattice,  $p=2\pi/24$ , the scaling curve increases as momentum decreases. From the non-symmetric lattice,  $16^3 \times 32$ , we can extract one data point corresponding to  $p_{min} = 2\pi/32$ . This point is found to lie below its neighbours. It is unlikely that this is due to finite size effects as the latter would enhance  $G(p)$ .

Therefore we are tempted to interpret this point as a genuine signal, that  $G(p)$  has a maximum somewhere inside the interval  $[\frac{2\pi}{32}, \frac{2\pi}{24}]$ .

It is comforting to observe a similar structure in our SU(2) data, at  $\beta=2.7$  (see Fig.2). The  $16^4$  and  $32^4$  data exhibits, after due normalization in configuration space, small finite size effects. Again, we observe (a) agreement of  $G(p=2\pi/16)$  as measured on the  $16^4$  and  $32^4$  lattices and (b) a turnover behaviour of  $G(p)$  at very small values of  $p$ .

We are thus led to the conclusion that there is no direct evidence for dipole dominance in our data.

One may expand  $G(p)$  in powers of  $1/q(p)^2$

$$G(p) = \frac{a}{q^2} + \frac{b}{q^4} + \dots, \quad (14)$$

and fit the data to the lowest terms. In the region of small momenta, we were forced to include terms up to  $\mathcal{O}(q^{-8})$ , in order to match the data. However, such fitting implies large cancellations of terms inducing substantial instabilities.

In the large momentum regime,  $q \geq \sqrt{2}$ , the data can be described by the first two terms in Eq.14. The fit yields the parameters quoted in Table 2. Obviously, the quadratic term  $\sim 1/q^2$  accounts for most of the tail in the distribution  $G(p)$ , the effective  $\simeq 1/q^4$  contribution being determined within 10% accuracy.

		a	b
SU(3)	$8^4$	0.746(8)	0.276(29)
	$16^3 \times 32(a)$	0.749(9)	0.227(33)
	$24^4$	0.744(10)	0.256(40)
SU(2)	$16^4$	2.073(12)	0.267(35)
	$32^4$	2.084(17)	0.299(45)

Table 2: *Fit parameter for the  $q \geq \sqrt{2}$  range, according to the ansatz 14.*

## 5 Conclusions

We have studied, for the first time, the ghost propagator for SU(2) and SU(3) pure gauge theories.

It appears that the gauge fixing algorithms used in the present study suffice to suppress the effects of Gribov copies. The performance of the SA algorithm for SU(2) is comparable to the ordinary relaxation algorithm in CPU time, but it has the advantage of finding the absolute minimum in a single run. The SOR, in combination with the Los Alamos algorithm, reduces the number of required iterations by nearly a factor 4, depending on  $w$  and on the lattice size. The extra cost for applying the “wrong” gauge transformation is negligible in comparison with the profit in iteration numbers.

The ghost propagators appear to be only little affected by finite size effects as we can verify from comparing the data from lattices of different extensions, at a given  $\beta$ .

In the infrared regime – measuring down to momentum values of 0.39 GeV and 0.86 GeV in SU(3) and SU(2), respectively – we do not confirm the expected

$1/q^4$  behaviour. Near the boundary of the first Brillouin zone,  $p \rightarrow \pi/L$ ,  $G(p)$  is dominated by  $1/q^2$ .

### Acknowledgments

We thank D. Zwanziger, who triggered this research, for useful discussions. This work was supported partially by DFG grants Schi 257/3-3, Schi 257/5-1, Pe 257/1-4 and EU network CHRX-CT92-0051 and by the Energy Research Group, University of Damascus, Syria.

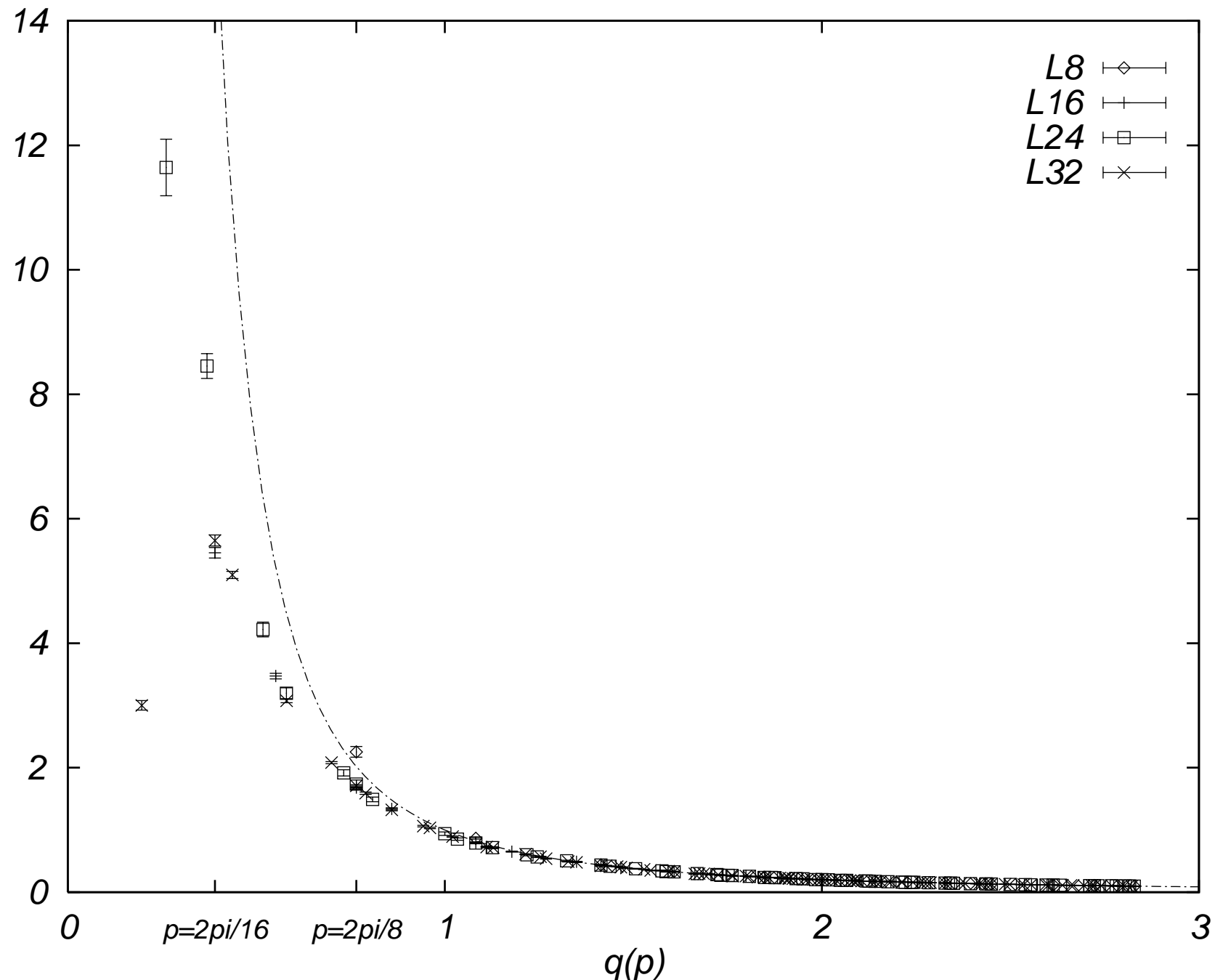
## References

- [1] M. Baker, J.S. Ball and F. Zachariasen, Nucl. Phys. B186 (1981) 531,560.
- [2] J.M. Cornwall, Phys. Rev. D26 (1982) 1453.
- [3] V.N. Gribov, Nucl. Phys. B139 (1978) 1.
- [4] D. Zwanziger, Nucl. Phys. B412 (1994) 657.
- [5] J.E. Mandula and M. Ogilvie, Phys. Lett. 185B (1987) 127.
- [6] C. Bernard, C. Parrinello and A. Soni, Phys. Rev. D49 (1994) 1585.
- [7] see e.g. A. Hulsebos, Nucl. Phys. B (Proc. Suppl.) 30 (1993) 539; H. Suman and K. Schilling, Parallel Computing 20 (1994) 975.
- [8] Ph. de Forcrand and R. Gupta, Nucl. Phys. B (Proc. Suppl.) 9 (1989) 516.

## Figure Captions

Figure 1:  $G(q)$  for  $SU(3)$  at  $\beta = 6.0$  on different lattice sizes. The curve represents the fit to the  $24^4$ -data according to the ansatz (Eq.14) in the range  $q \geq \sqrt{2}$ . Note that the full  $q$ -range in our simulation is given by  $0 \leq q \leq 2\sqrt{2}$ .

Figure 2: The same as Fig. 1, but for  $SU(2)$  at  $\beta=2.7$ . The fit shown is for the  $32^4$  lattice.

$G(q)$ 

$G(q)$ 